Theoretical Insights into the Role of a Counterion in Copper–Catalyzed Enantioselective Cyclopropanation Reactions

ARTICLE *in* CHEMISTRY · FEBRUARY 2004

Impact Factor: 5.73 · DOI: 10.1002/chem.200305161 · Source: PubMed

6 AUTHORS, INCLUDING:

José M Fraile
University of Zaragoza
192 PUBLICATIONS **3,849** CITATIONS
SEE PROFILE

José I García
Spanish National Research Council
264 PUBLICATIONS **4,992** CITATIONS
SEE PROFILE

Víctor Martínez-Merino
Universidad Pública de Navarra
67 PUBLICATIONS **1,124** CITATIONS
SEE PROFILE

Alba Mayoral
University of Alcalá
114 PUBLICATIONS **1,917** CITATIONS
SEE PROFILE

Theoretical Insights into the Role of a Counterion in Copper-Catalyzed Enantioselective Cyclopropanation Reactions

José M. Fraile,[a] José I. García,*[a] María J. Gil,[b] Víctor Martínez-Merino,*[b] José A. Mayoral,[a] and Luis Salvatella[a]

Abstract: The effect of a coordinating counteranion on the mechanism of Cu^{I}-catalyzed cyclopropanation has been investigated extensively for a medium-sized reaction model by means of theoretical calculations at the B3LYP/6-31G(d) level. The main mechanistic features are similar to those found for the cationic (without a counteranion) mechanism, the rate-limiting step being nitrogen extrusion from a catalyst–diazoester complex to generate a copper–carbene intermediate. The cyclopropanation step takes place through a direct carbene insertion of the metal–carbene species to yield a catalyst–product complex, which can finally regenerate the starting complex. However, the presence of the counteranion has a noticeable influence on the calculated geometries of all the intermediates and transition structures. Furthermore, the existence of a preequilibrium with a dimeric form of the catalyst, together with a higher activation barrier in the insertion step, explains the lower yield of cyclopropane products observed experimentally in the presence of chloride counterion. The stereochemical predictions of a more realistic model (made by considering a chiral bis(oxazoline)–copper(I) catalyst) have been rationalized in terms of the lack of significant steric repulsions, and the model shows good agreement with the low enantioselectivities observed experimentally for these kinds of catalytic systems.

Keywords: asymmetric catalysis · copper · cyclopropanation · density functional calculations · ligand effects · N ligands

Introduction

Cyclopropane derivatives are an important family of chemical compounds because of their interesting biological properties[1] as well as their use as starting materials and intermediates in organic synthesis.[2] Great efforts have therefore been made to develop efficient diastereo- and enantioselective methods for the synthesis of cyclopropanes.[3] A particularly versatile method is metal-catalyzed cyclopropanation of olefins with diazo compounds, for which various efficient homogeneous catalysts have been developed.

[a] Dr. J. M. Fraile, Dr. J. I. García, Dr. J. A. Mayoral, Dr. L. Salvatella
Departamento de Química Orgánica
Instituto de Ciencia de Materiales de Aragón
C.S.I.C.-Universidad de Zaragoza
Pedro Cerbuna 12, 50009 Zaragoza (Spain)
Fax: (+34) 976762077
E-mail: jig@unizar.es

[b] Dr. M. J. Gil, Dr. V. Martínez-Merino
Departamento de Química Aplicada
Universidad Pública de Navarra, 31006 Pamplona (Spain)
Fax: (+34) 948169606
E-mail: merino@si.unavarra.es

Supporting information for this article is available on the WWW under http://www.chemeurj.org/ or from the author.

The use of catalysts based on copper is particularly attractive because of their high efficiency in asymmetric cyclopropanation reactions[4] and their relatively low cost in comparison with other metal derivatives, such as catalysts based on rhodium[5] or ruthenium.[6] Various chiral ligands have been described for the enantioselective versions of the cyclopropanation reaction, including salicylaldimines,[7] salicylaldehyde–amino acid derivatives,[8] and semicorrins.[9] The best results have been obtained with bis(oxazolines)—described independently by Evans and co-workers[10] and Masamune and co-workers[11]—which can lead to almost complete enantioselectivity (up to 99% *ee*) when their complexes with Cu^{I} or Cu^{II} are used in cyclopropanation reactions. Good performance of chiral bis(oxazolines) as ligands for asymmetric cyclopropanation, as well as for other Lewis acid catalyzed reactions, has resulted in the recent commercial availability of some of them.

For large-scale applications, the ease of use and facile recovery of the chiral catalysts have become important factors; several studies have focused on the immobilization of chiral Cu complexes for catalytic cyclopropanation reactions.[12] However, in both the homogeneous[10,13] and heterogeneous[14] phases, a dramatic dependence of the stereoselectivity on factors such as the solvent and the counterion has been described. For instance, Evans et al. have report-

DOI: 10.1002/chem.200305161

ed[10] that the use of halides, cyanide, acetate, or perchlorate counteranions leads to a decreasing or even a total loss of catalytic activity, and to a noticeable decrease in enantioselectivity. In particular, when the counteranion is changed from triflate to chloride, the enantioselectivity of the cyclopropanation reaction of styrene with ethyl diazoacetate, catalyzed by the 2,2′-isopropylidenenebis[(4*S*)-*tert*-butyl-2-oxazoline]–copper(I) complex in dichloromethane, drops from 94 to 3% *ee* for the *trans*-cyclopropanes, and from 92 to 8% *ee* for *cis*-cyclopropanes.[13] The origin of this behavior still remains unclear.

Several thorough theoretical studies[15–17] concerning the mechanism of the copper-catalyzed cyclopropanation reactions of diazo compounds have been published recently. We present here a theoretical study dealing with the effect of the counterion of the catalytic complex on the mechanism of the cyclopropanation reaction and its consequences for the enantioselectivity.

Results and Discussion

Computational methods: In our previous work,[15] a relatively simple nonchiral model of the catalytic complex, namely the *N*,*N*′-dimethyl malonaldiimine–copper(I) cation (**1**) (Scheme 1), was used to explore the potential energy surface

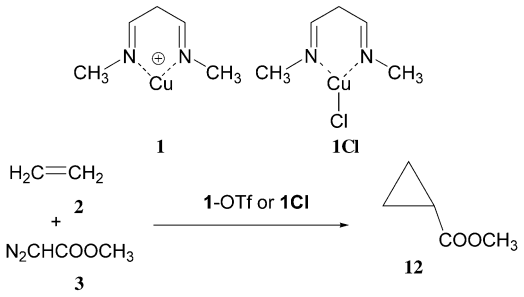

Scheme 1. Model Cu-catalyzed cyclopropanation reaction.

thoroughly by considering different reaction pathways. Such a model is positively charged due to the well-known weak coordinating ability of the triflate counteranion in solution.[18] The effect of a strong coordinating counteranion has been taken into account by using the same model, but with a chloride anion linked to the copper center (**1Cl**) so that the resulting system is neutral (Scheme 1). The model reaction chosen was the cyclopropanation of ethylene (**2**) with methyl diazoacetate (**3**) (Scheme 1). We have taken the possibility of different conformations into account for all structures, although we center our discussion of the results on the most stable form in each case.

All calculations were performed by means of the B3LYP hybrid functional[19] because this technique has performed satisfactorily in the chemistry of transition metals[20] and, in particular, in our previous work.[15] Full optimizations using the 6-31G(d) basis set for all the atoms were carried out using the Gaussian 98 package.[21] BSSE corrections were not considered for this work.

Analytical frequencies were calculated at the B3LYP/6-31G(d) level and the nature of the stationary points was determined in each case according to the appropriate number of negative eigenvalues in the Hessian matrix. Scaled frequencies were not considered since significant errors on the calculated thermodynamic properties are not found at this theoretical level.[22]

In selected cases, single-point energy calculations were carried out with the extended triple zeta split-valence 6-311++G(2d,p) basis set. Solvent effects were also taken into account in selected cases by the IPCM method,[23] as implemented in Gaussian 98. The dielectric permittivity of dichloromethane ($\varepsilon = 8.93$) was used, with an isodensity cut-off value of 0.0001.

Unless otherwise stated, only Gibbs free energies are used in the discussion of the relative stabilities of the chemical structures considered. Relative free energies (including thermal corrections at 25 °C) of the structures considered for the nonchiral model are shown in Table 1. Hard data on electronic energies, entropies, Gibbs free energies, and lowest frequencies of the different conformations of all the structures considered are available as Supporting Information.

Table 1. Numbering and relative Gibbs free energies [kcal mol^{-1}] of the different nonchiral structures considered in this work.

Structure	$\Delta\Delta G$[a]	$\Delta\Delta G_{PCM}$[b]
2	0.0	0.0
3	0.0	0.0
4	0.0	0.0
1Cl	6.6	6.8
(1Cl)$_2$	−10.8	−2.0
5Cl	0.0	0.0
6Cl	8.8	10.7
7Cl	20.7	23.3
8Cl	−2.6	0.0
9Cl	10.2	13.1
10Cl	−30.0	–
11Cl	−24.8	–
12	−51.9	−51.2
13Cl	0.4	3.4
14Cl	−13.1	−10.2

[a] Calculated at the B3LYP/6-31G(d) theoretical level (298 K). [b] Calculated at the IPCM/B3LYP/6-31G(d)//B3LYP6-31G(d) theoretical level, using the B3LYP/6-31G(d) frequencies (298 K).

Formation of the copper–carbene complex: Figure 1 shows the calculated structures for the initial complex **1Cl**, togeth-

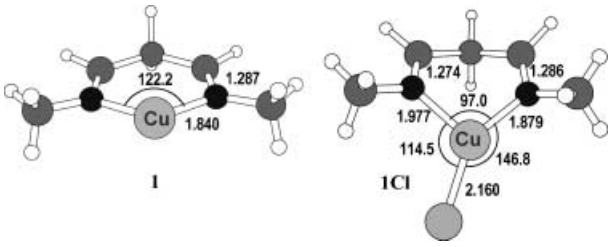

Figure 1. Structures of the catalyst without (**1**) and with (**1Cl**) the chloride counterion. Distances in all figures are in Å.

er with the structure of the corresponding cationic species[15] for comparison.

The cationic species is fully planar, whereas the neutral complex **1Cl** exhibits a boat conformation. The Cu atom presents a trigonal-planar coordination, but the Cu–Cl bond deviates considerably from the central axis of the chelate complex, with unequal N-Cu-Cl bond angles of 114.5° and 146.8°. As a consequence, the whole complex is asymmetric and, for instance, the N–Cu coordination bonds are 1.879 and 1.977 Å, respectively, for the bonds *anti* and *syn* to the chlorine atom. Both bonds are longer than those calculated for the cationic complex **1**, which indicates a weaker coordination of the diimine ligand to the Cu center. This is undoubtedly attributable to the presence of a more electron-deficient Cu center in **1**.

Since the Cu atom bears a chlorine ligand, fewer possible intermediate and transition structures are expected to exist than positively charged species, which have an additional coordinative vacancy. Indeed, intermediate complexes with two reactive molecules simultaneously coordinated to the Cu center were not localized in any case. However, a dimeric structure of **1Cl**, denoted as **$(1Cl)_2$**, could be located and characterized as a minimum. The structure of this dimer is shown in Figure 2, along with those of intermediate complexes bearing another coordinated reactive molecule (**5Cl** and **6Cl**) together with their cationic counterparts.[15] The formation of dimeric species through di-μ-X bridges (where X is the anion) would be specially suitable when $X = Cl^-$, but much more difficult, and even impossible, in the case of other anions such as perchlorate or cyanide. Consequently, a general mechanistic explanation of the counteranion effect in the reaction should not be based entirely on the formation of dimeric species (see below).

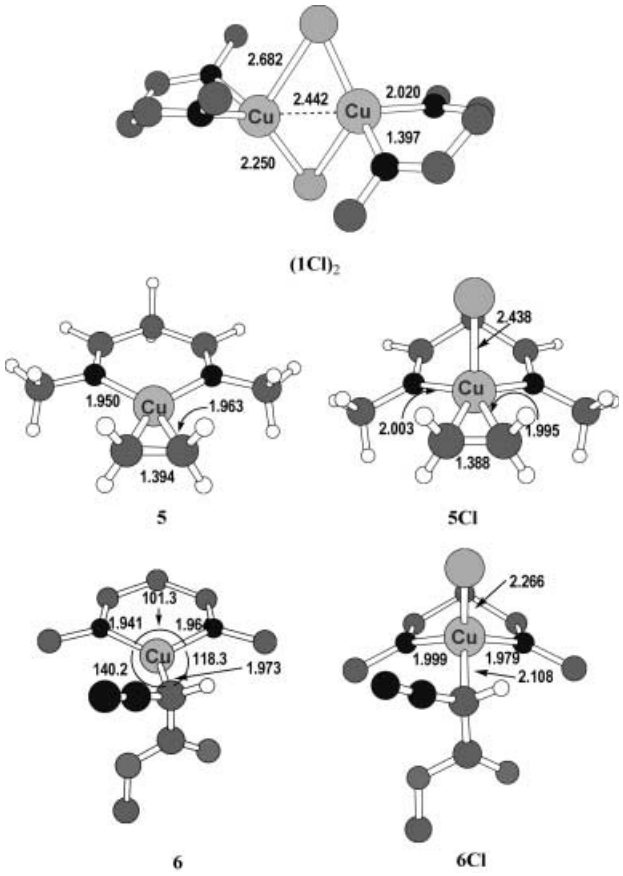

Figure 2. Structures of the **1Cl** dimer, **$(1Cl)_2$**, and the intermediate complexes with an ethylene (**5** and **5Cl**) or a diazo ester molecule (**6** and **6Cl**) coordinated to the Cu center. Some hydrogen atoms have been omitted for clarity.

The presence of the chloride counterion introduces marked changes in the molecular structures of these intermediates. For example, whereas complex **5** presents a square-planar coordination, complex **5Cl** is pyramidal. Furthermore, similarly to the parent complexes **1** and **1Cl**, the diimine–Cu complex is fully planar for **5**, whereas it adopts a boatlike conformation for **5Cl**. Similar characteristics can be highlighted for complexes **6** and **6Cl**. In these cases, the coordination geometry changes from distorted trigonal planar (**6**) to tetrahedral (**6Cl**) when the coordination of the counterion is taken into account. In all cases, the coordination bonds of both the diimine ligand (N–Cu bonds) and the reactives (C–Cu bonds) are significantly longer in the neutral complexes than in their cationic counterparts, a situation that indicates greater electron demand in the latter. Accordingly, the Cl–Cu bond is also longer in these intermediates, due to the electron donation of the reactives. The greater bond length of 2.438 Å found for **5Cl**, which indicates strong π donation due to the ethylene ligand, is noteworthy.

The first transition structure (TS) found on the reaction coordinate corresponds to dinitrogen extrusion from complex **6Cl**. Some geometrical features of this TS (**7Cl**) are presented in Figure 3. The differences found for the complexes described previously, that is, ring conformation and coordination bond lengths, are also observed for the cationic counterpart **7**. Dinitrogen dissociation results in strengthening of the C_α–Cu bond in the intermediate complex **6Cl**, as illustrated by the reduction in the corresponding bond length from 2.108 to 1.870 Å. At the same time, this situation leads to a weakening of one of the N–Cu bonds and the Cl–Cu bond, as shown by the increase in the corresponding bond lengths (from 1.999 to 2.056 Å for N–Cu, and from 2.266 to 2.376 Å for Cl–Cu).

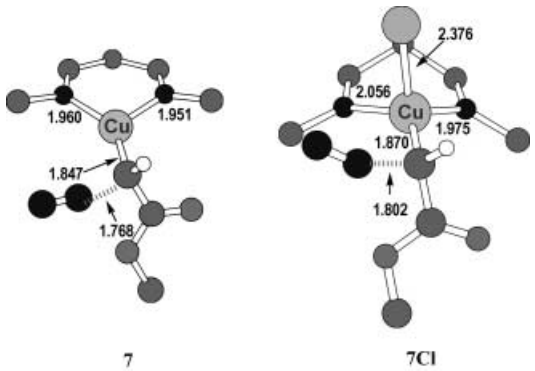

Figure 3. Structures of the transition structures for dinitrogen extrusion with (**7Cl**) and without (**7**) the chloride counterion. Some hydrogen atoms have been omitted for clarity.

The extrusion of dinitrogen is followed by formation of the the Cu–carbene complex. The key importance of this intermediate has recently been shown both theoretically[15,17] and experimentally.[24] The calculated structure for this complex (**8Cl**) is shown in Figure 4. Apart from the boatlike

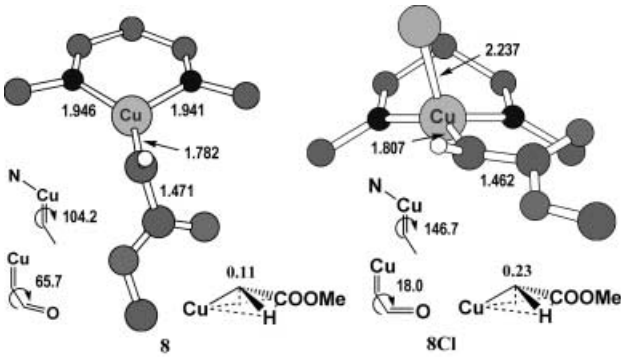

Figure 4. Structures of the Cu–carbene units with (**8Cl**) and without (**8**) the chloride counterion. Some hydrogen atoms have been omitted for clarity.

conformation of the chelate complex, a major difference is observed between complexes **8** and **8Cl** in the spatial disposition of the ester group relative to the complex. For the cationic complex **8**, the carbene-carbon–Cu bond is almost perpendicular to the plane of Cu–diimine complex and it is also perpendicular to the plane of the ester group. This situation can be attributed to the strong electrophilic character of this carbene-carbon atom, which avoids coplanarity with electron-withdrawing groups. The geometry of the carbene-carbon atom indicates sp^2 hybridization, which causes a very small deviation from coplanarity (0.11 Å).

In **8Cl**, however, the carbene-carbon atom is more nearly coplanar with both the plane of Cu–diimine complex and that of the ester group. Furthermore, this carbon atom is somewhat more pyramidalized, with a deviation of 0.23 Å from planarity.

The N–Cu bonds are longer in **8Cl** than in **8**, analogously to the calculated structures already mentioned. This indicates that the coordination of the diimine ligand to the Cu center is weaker, because of the presence of the chloride counterion. This raises the question of whether the diimine ligand in **8Cl** could be dissociated to a significant extent; this would have important implications for the stereoselectivity in the case of a chiral ligand. To answer this question, the equilibrium represented by Equation (1) was calculated

$$\mathrm{Cl{-}Cu{=}CHCOOMe} \; + \; \mathrm{diimine} \rightleftharpoons \mathbf{8Cl} \qquad (1)$$

(full results are available in the Supporting Information). The formation of **8Cl** is favored by 19.1 kcal mol^{-1} in terms of Gibbs free energy; this increases to 20.7 kcal mol^{-1} when solvent effects are taken into account. Another possible mechanism through which nonchiral catalytic species could be formed is the formation of a dimeric $(\mathrm{Cl{-}Cu{=}CHCOOMe})_2$ species through two di-μ-Cl bridges, by the equilibrium in Equation (2). However, the formation of this

$$2\,\mathbf{8Cl} \rightleftharpoons 2\,\mathrm{diimine} \; + \; (\mathrm{Cl{-}Cu{=}CHCOOMe})_2 \qquad (2)$$

species is disfavored in terms of Gibbs free energy by 17.7 kcal mol^{-1}, which increases to 24.5 kcal mol^{-1} when solvent effects are taken into account. We therefore rule out the possibility of a significant contribution by noncoordinated Cu species to the reaction pathway.

The geometrical differences between the key **8Cl** intermediate and **8** have important consequences for the shape and orientation of the corresponding LUMO (Figure 5). For

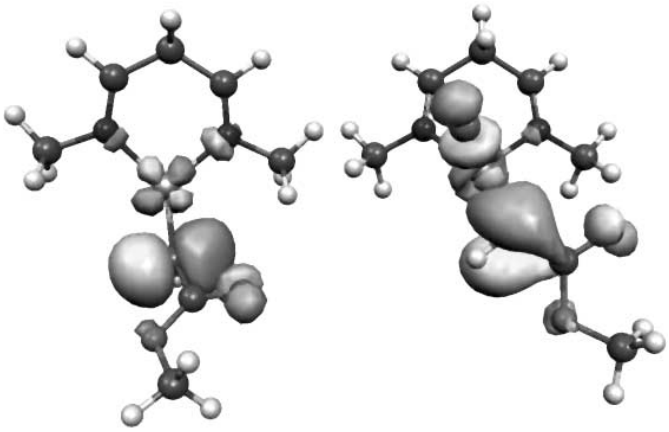

Figure 5. Isocontour plots (0.005 a.u.) of the LUMO of the Cu–carbene complexes **8** and **8Cl**, calculated at the B3LYP/6-31G(d) theoretical level.

example, for **8** the main LUMO lobe is centered on the carbene-carbon atom and it points in a direction that is coplanar with the Cu–diimine plane. In **8Cl**, however, slight conjugation between the carbene and the carboxyl carbon atoms is observed, and the main LUMO lobe points in a direction perpendicular to the Cu–diimine plane. Both situations should have important implications for the geometry of the transition states for the insertion of the carbene into the alkene double bond (see below).

Formation of the cyclopropane products: We established previously[15] that the direct insertion of the carbene into the alkene double bond is favored over the metallacyclobutane pathway. Both reaction pathways were also investigated in the presence of the chloride counteranion. Figure 6 shows the transition structures for the direct insertion for both the cationic (**9**) and the neutral (**9Cl**) pathways.

Two main features distinguish between the two transition structures. First, for **9** the ethylene approaches in the plane of the complex, whereas for **9Cl** it approaches from a direction close to that of the Cu–Cl bond (the dihedral angle between the middle of the ethylene double bond, the carbene-carbon atom and the Cu–Cl bond is approximately 30°). These directions of approach are in agreement with the calculated geometries of the Cu–carbene LUMOs (Figure 5). However, when we tested other directions of approach for **9Cl**, particularly those in which the groups are rotated so

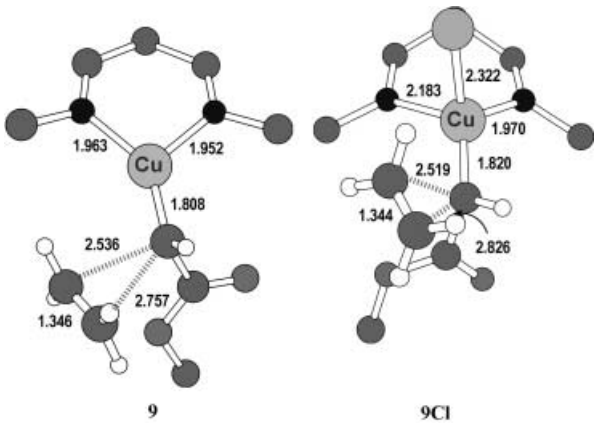

Figure 6. Transition structures for the direct insertion of the carbene into the ethylene double bond, with (**9Cl**) and without (**9**) the chloride counterion. Some hydrogen atoms have been omitted for clarity.

that the Cu–Cl bond is opposite the carbene insertion, we were unable to obtain converged structures for any of the corresponding TS. Second, the degree of asynchronicity is greater in **9Cl** than in **9**.

The second possible reaction pathway involves the formation of a cupracyclobutane intermediate with subsequent evolution to the cyclopropane product. However, although such an intermediate could be located in the potential energy surface (Figure 7), extensive searches failed to reveal

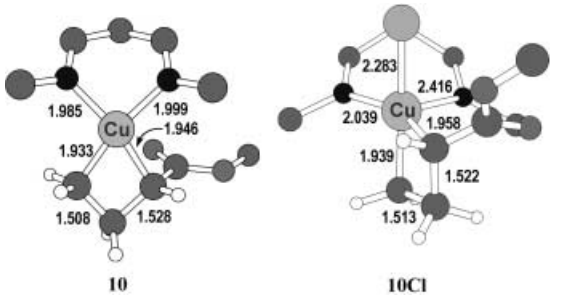

Figure 7. Structures of the cupracyclobutane intermediates with (**10Cl**) and without (**10**) the chloride counterion. Some hydrogen atoms have been omitted for clarity.

a transition structure connecting the Cu–carbene complex **8Cl** with the cupracyclobutane **10Cl**. Systematic energy scans led to a continuous energy rise as the ethylene molecule approached **8Cl** with its carbon atoms pointing to the Cu and the carbene carbon atoms, respectively. However, a transition structure (**11Cl**) was found that corresponds to the transformation of **10Cl** into the cyclopropane product (**12**). Therefore it can be concluded that, in the presence of a strong coordinating counteranion, the only reaction pathway available is the direct, concerted insertion of the carbene into the double bond—with the hypothetical existence of a cupracyclobutane representing a dead end in the reaction coordinate.

The presence of the chloride counterion also has a marked effect on the geometry of the cupracyclobutane intermediates. For example, whereas the cationic complex has a square-planar geometry, the neutral complex displays a trigonal-bipyramidal structure in which the cupracyclobutane ring is perpendicular to the Cu–diimine plane.

A referee proposed a different mechanism, similar to that described for the Simmons–Smith cyclopropanation.[25] The first step of this mechanism would be the 1,2 migration of the chlorine atom from Cu to the carbene carbon; in fact, both the transition structure for this migration (**13Cl**) and the resulting carbenoid complex (**14Cl**) could be located and properly characterized (Figure 8).

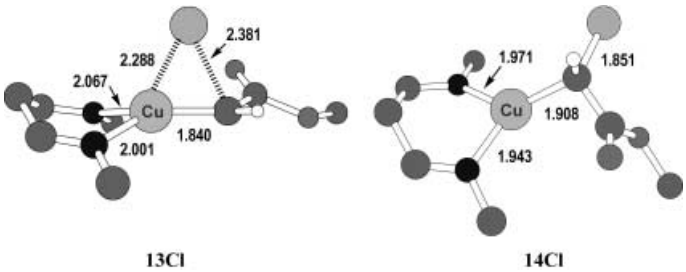

Figure 8. Transition structure for the 1,2 chlorine shift from Cu to the carbene carbon of **10Cl** (**13Cl**) and structure of the resulting carbenoid complex (**14Cl**).

However, an examination of the LUMO of the carbenoid complex **14Cl** revealed that this orbital does not possess the correct symmetry to be involved in the reaction. Indeed, only the LUMO+3 (more than 2 eV higher in energy than the LUMO) has a significant orbital lobe centered on the carbenoid carbon. This seems to indicate that this species has a low reactivity towards the insertion into the double bond of an olefin. After extensive searches, we were unable to locate either a transition structure similar to those involved in the Simmons–Smith cyclopropanation reactions, or a four-center transition structure involving the Cu atom. Therefore, we conclude that these kinds of carbenoid species do not contribute to the reaction mechanism in the Cu-catalyzed reactions.

Energy considerations: The relative free energies of the structures shown in the energy diagram (Figure 9) take into account the evolution of the system composition according to the different molecules entering or leaving the system. The catalytic intermediate **5Cl**, ethylene (**2**), methyl diazoacetate (**3**), and dinitrogen (**4**) have been chosen arbitrarily as reference points for the calculation of relative free energies (Table 1).

In both cases the formation of the Cu–carbene complex is the rate-determining step, a situation in agreement with the experimental observations in related systems,[26] since it has the highest activation barrier over the whole reaction coordinate. However, the reaction pathway is somewhat different for the neutral and the cationic complexes. The high relative energy of complex **1** prevents a dissociative mechanism for the transition from **5** to **6**.[15] For the neutral pathway, the presence of the chloride prevents an associative ligand mechanism, but the relative energy of **1Cl** allows the dissociative mechanism for the transition from **5Cl** to **6Cl**. If we calculate the activation barrier for this step from **5Cl**, the

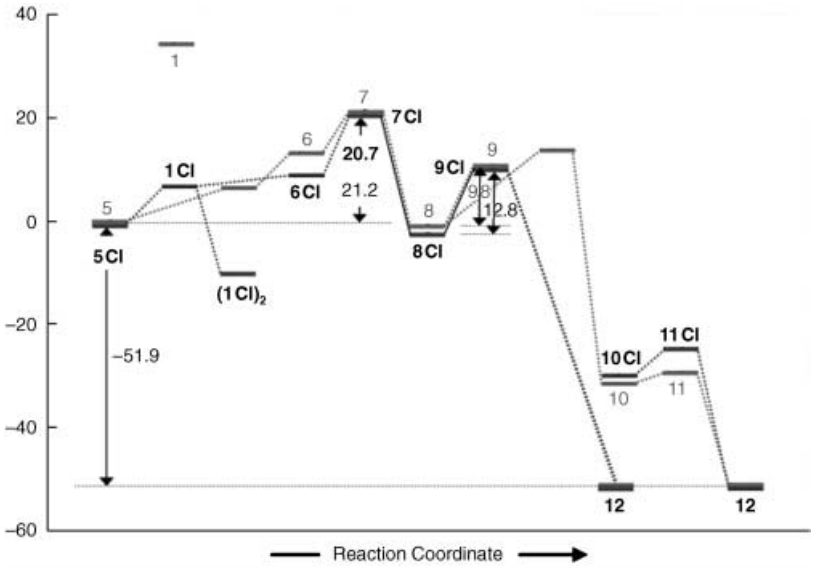

Figure 9. Free-energy diagram for a catalytic cycle of the cationic (——) and the neutral (·····) complexes. Energy values are in kcal mol^{-1}.

value obtained (approximately 21 kcal mol^{-1}) is very similar in both cationic and neutral pathways. Given that stronger solvent effects should be expected for the cationic species, we estimated the solvation energies of the principal species involved in this step by some single-point calculations (Table 1). Somewhat surprisingly, the activation barriers are only slightly modified, even in the case of the cationic complexes. This indicates the existence of only a small differential solvation between the transition structures and the reactives. Thus, the activation barrier of the cationic pathway increases from 21.1 (gas phase) to 25.0 kcal mol^{-1} (dichloromethane), whereas for the neutral pathway the increase is somewhat lower, from 20.7 (gas phase) to 23.3 kcal mol^{-1} (dichloromethane). Therefore the significant decrease in the yield of cyclopropane products observed with coordinating counteranions such as chloride, in comparison with triflate and other weakly coordinating counteranions,[13] does not seem to be due to a direct influence of the counteranion on the activation barrier of the rate-determining step.

However, the presence of a chlorine atom allows other possibilities that should be examined; the dimerization of **1Cl**, as previously mentioned, is the most feasible. The calculated free energy of formation of **(1Cl)$_2$** from **1Cl** is -10.8 kcal mol^{-1} in the gas phase, and decreases to -2.0 kcal mol^{-1} when solvent effects are taken into account. This indicates that a preequilibrium [Eq. (3)] is feasible,

$$2\,\mathbf{1Cl} \rightleftharpoons (\mathbf{1Cl})_2 \qquad (3)$$

and therefore the activation barrier for the N_2 extrusion should be calculated from **(1Cl)$_2$** and not from **5Cl** (Figure 9), leading to a value of approximately 32 kcal mol^{-1} in the gas phase, and of 23.2 kcal mol^{-1} when solvation energies are included. This circumstance would result in a decrease in the apparent rate kinetic constant. However, as stated above, this situation will hold only with counteranions able to give such dimeric species. Another possible, and probably more general, mechanism for the observed decrease in yield is the easier formation of by-products (see below).

The activation barrier for the insertion step is 9.8 kcal mol^{-1} on the cationic pathway, whereas it increases to 12.8 kcal mol^{-1} for the neutral pathway. However, in the latter case solvent effects have a leveling effect on the barriers and, when differential solvation energies are taken into account, the corresponding activation energies change to 12.0 and 13.1 kcal mol^{-1}, respectively. The higher barrier in the case of the neutral pathway would favor the formation of by-products such as maleates or fumarates, or even the pyrazolines derived from the 1,3 dipolar cycloaddition between the diazo ester and these products.[13] All of these processes would result in a lower styrene conversion, which is in agreement with experimental observations.[13]

All the reaction pathways show almost parallel development across most of the reaction coordinate. Therefore, although the chloride counterion significantly influences the structures of the intermediates and the transition structures, the reaction mechanism remains essentially unchanged with respect to the cationic pathway (which represents the situation with a weakly coordinating counteranion). The activation energies of the principal steps are also similar, irrespective of the presence or absence of a counterion.

Extension to a chiral model: To pursue our interest in the effect of the counterion on the enantioselectivity, we extended the theoretical study to include a chiral model. As the chiral ligand we chose the simplified bis(oxazoline) structure used previously,[15] namely 2,2′-methylenebis[(4*S*)-methyl-2-oxazoline]. The presence of the chloride counteranion together with a chiral ligand led to different possible Cu^{I}–carbene complexes, which were calculated at the B3LYP/6-31G(d) theoretical level. The optimized structure of the resulting minimum-energy structure is shown in Figure 10.

The Cu–carbene complex **15Cl** displays most of the features already described for the nonchiral complex **8Cl**. This complex has a boatlike conformation in the Cu–diimine complex and a tetrahedral Cu center; in addition, the disposition of the carbene carbon is more coplanar with regard to both the Cu–diimine complex and the ester group—unlike the situation in cationic complex **15**. As a consequence, the main lobe of the LUMO will point in a direction perpendicular to the principal plane of the complex.

The complexation free energy of the equilibrium represented by Equation (4) was calculated, similarly to that al-

$$\mathrm{Cl{-}Cu{=}CHCOOMe} + \mathrm{bis(oxazoline)} \rightleftharpoons \mathbf{15Cl} \qquad (4)$$

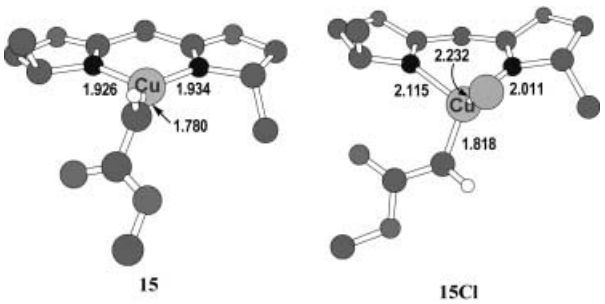

Figure 10. Structures of the Cu–carbene intermediates with (**15Cl**) and without (**15**) the chloride counterion. Some hydrogen atoms have been omitted for clarity.

ready described in the case of the nonchiral model. The formation of the complex is favored by approximately 25 kcal mol^{-1} (28.6 kcal mol^{-1} if solvent effects are taken into account), which clearly rules out the possibility of a nonchiral reaction pathway.

The transition structures corresponding to the approach of ethylene at the *Re* (**16Cl**) and *Si* (**17Cl**) faces of the carbene carbon were also calculated at the same level. The resulting geometries are shown in Figure 11.

The structures of **16Cl** and **17Cl** show only small differences from that calculated for the nonchiral model (**9Cl**). Thus, whereas **17Cl** is later than **9Cl**, as indicated by the shorter C–C bond-forming distances and the longer ethylene C–C bond length, **16Cl** is earlier. When we consider the direction of approach of ethylene, the dihedral angles between the middle of the ethylene double bond, the carbene-carbon atom and the Cu–Cl bond are above and below that calculated for **9Cl** (**16Cl**: 20°; **17Cl**: approximately 40°. In comparison with the Cu–carbene intermediate **15Cl**, the carbene-carbon atom appears twisted by about 120°, implying that the ethylene approaches on the same side of the Cu–Cl bond. Other properly converged structures could not be found for these TS. Indeed, even when the starting structures had the approaching ethylene molecule on the opposite side to the chlorine atom, the calculation converged to structures **16Cl** and **17Cl**.

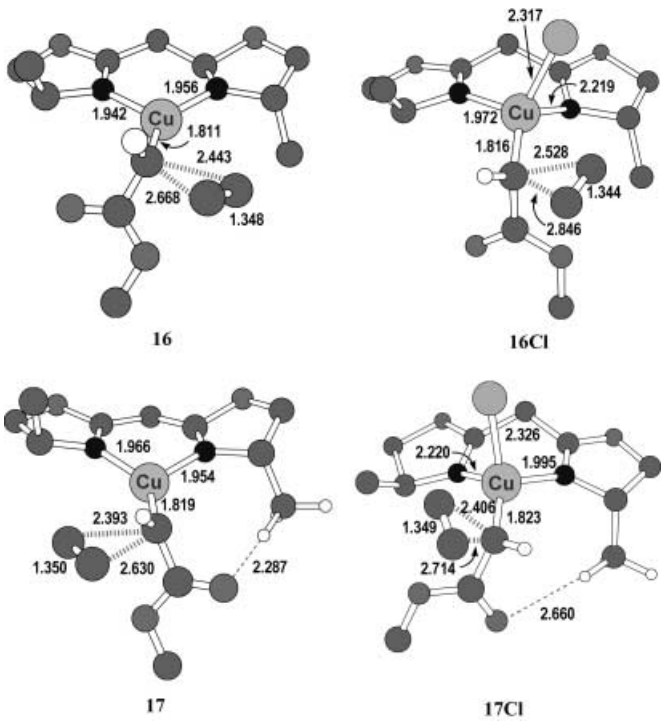

Figure 11. Transition structures of the cyclopropanation step for the attack of ethylene at the *Re* (**16** and **16Cl**) and *Si* (**17** and **17Cl**) faces of the chiral catalyst–carbene complex. Some hydrogen atoms have been omitted for clarity.

Further significant differences can be seen when the neutral TS is compared with the cationic TS. For instance, the two N–Cu bonds in the complexes are longer but more unsymmetrical in the neutral complexes (**16Cl** and **16**: Δd = 0.247 and 0.014 Å; **17Cl** and **17**: Δd = 0.225 and 0.012 Å). The Cu–$C_{carbene}$ bonds are also somewhat longer in the neutral complexes.

There are also important structural differences that could be crucial for the asymmetric induction. The main steric interaction responsible for the enantioselection has been determined[15,16] to be that between the carbonyl-oxygen atom of the ester group and the substituent on one of the stereogenic carbon atoms of the bis(oxazolines), in agreement with Pfaltz's suggestion.[4] Indeed, a short distance (2.287 Å) between these groups was calculated for the cationic complexes, a fact that explains the instability of **17** relative to **16**. For the neutral complex **17Cl**, the distance calculated between the same atoms is noticeably longer (2.660 Å). Furthermore, there are no other significant close contacts in either **16Cl** or **17Cl**. This fact should have important consequences for the relative energies of the two TS.

At the B3LYP/6-31G(d) level, **16Cl** is favored over **17Cl** by 0.7 kcal mol^{-1}. This margin decreases to only 0.4 kcal mol^{-1} when a larger basis set (6-311++G(2d,p)) is considered. For comparison, the corresponding values found[15] for **16** and **17**, are 2.6 and 1.9 kcal mol^{-1}, respectively. The energy results are therefore in agreement with the lack of clear steric interactions that are able to distinguish the diastereomeric TS in the case of the neutral pathway. Solvent effects were also considered in this case and, when account is additionally taken of differential solvation of the TS (by means of IPCM/B3LYP/6-31G(d) single-point energy calculations), the calculated relative free energies of **16Cl** and **17Cl** increase to 0.8 kcal mol^{-1}, a value still below the 1.3 kcal mol^{-1} calculated for **16** and **17**.[15]

Conclusion

Theoretical calculations carried out on a simplified, nonchiral model show that the presence of a coordinating counteranion has important consequences in the geometries of the reaction intermediates and transition structures, but not in the overall reaction mechanism or the main reaction pathway. The rate-determining step is dinitrogen extrusion to give the Cu–carbene intermediate complex. The cyclopropane product is formed through the direct, concerted insertion of the carbene-carbon atom into the alkene double bond similarly to the mechanism reported for the cationic

(without counteranion) pathway. The main effect of the chloride counteranion is to reduce the chemoselectivity towards cyclopropane products. This reduction occurs in favor of carbene dimerization through a higher alkene insertion activation barrier and also probably through a preequilibrium with a dimeric form of the catalyst precursor, which in turn leads to a lower apparent kinetic rate constant.

Theoretical calculations on a chiral bis(oxazoline)–Cu model in the presence of a coordinating counteranion provide an explanation for the dramatic decrease in enantioselectivity observed experimentally when chloride, rather than triflate, is used as the counterion. The diastereomeric transition structures for the carbene insertion lack any clear steric interaction that is able to discriminate between the two prochiral faces of the carbene-carbon atom. This situation is due to the significant geometric changes induced by the presence of the chloride anion and is very different from that found for the cationic pathway. The calculated energy values for the insertion step agree well with a lower enantioselectivity in the presence of a coordinating counteranion.

One interesting conclusion from these findings is that the geometry of the chelate bis(oxazoline)–Cu complex (planar for the cationic pathway and boatlike for the neutral pathway) has a dramatic influence on the enantioselectivity of the cyclopropanation reactions. Therefore, other factors that are able to modify the geometry, like the substitution pattern on the bis(oxazoline) ligand, should also influence the stereochemical course of the reaction. Current theoretical studies in this area will be reported in due course.

Acknowledgments

This work was made possible by the generous financial support of the Comisión Interministerial de Ciencia y Tecnología (Project PPQ2002-04012) and the Diputación General de Aragón (Grupo consolidado, 2002–3).

[1] C. J. Suckling, *Angew. Chem.* **1988**, *100*, 555–570; *Angew. Chem. Int. Ed. Engl.* **1988**, *27*, 537–552.
[2] H. N. C. Wong, M.-Y. Hon, C.-W. Tse, Y.-C. Yip, J. Tanko, T. Hudlicky, *Chem. Rev.* **1989**, *89*, 165–198.
[3] a) T. Ye, M. A. McKervey, *Chem. Rev.* **1994**, *94*, 1091–1160; b) V. K. Singh, A. D. Gupta, G. Sekar, *Synthesis* **1997**, 137–149; c) M. P. Doyle, M. N. Protopopova, *Tetrahedron* **1998**, *54*, 7919–7946.
[4] a) A. Pfaltz in *Comprehensive Asymmetric Catalysis, Vol. 2* (Eds.: E. N. Jacobsen, A. Pfaltz, H. Yamamoto), Springer-Verlag, Berlin, **1999**, pp. 513–538; b) W. Kirmse, *Angew. Chem.* **2003**, *115*, 1120–1125; *Angew. Chem. Int. Ed.* **2003**, *42*, 1088–1093.
[5] K. M. Lydon, M. A. McKervey in *Comprehensive Asymmetric Catalysis, Vol. 2* (Eds.: E. N. Jacobsen, A. Pfaltz, H. Yamamoto) Springer, Berlin, **1999**, pp. 539–580.
[6] A. B Charette, H. Lebel in *Comprehensive Asymmetric Catalysis, Vol. 2* (Eds.: E. N. Jacobsen, A. Pfaltz, H. Yamamoto) Springer, Berlin, **1999**, pp. 581–603.
[7] H. Nozaki, S. Moriuti, H. Takaya, R. Noyori, *Tetrahedron Lett.* **1966**, *7*, 5239–5244.
[8] T. Aratani, *Pure Appl. Chem.* **1985**, *57*, 1839–1844.
[9] U. Leutenegger, G. Umbricht, C. Fahrni, P. Matt, A. Pfaltz, *Tetrahedron* **1992**, *48*, 2143–2156.
[10] D. A. Evans, K. A. Woerpel, M. M. Hinman, M. M. Faul, *J. Am. Chem. Soc.* **1991**, *113*, 726–728.
[11] R. E. Lowenthal, A. Abiko, T. Masamune, *Tetrahedron Lett.* **1990**, *31*, 6005–6008.
[12] a) J. M. Fraile, J. I. García, J. A. Mayoral, T. Tarnai, *Tetrahedron: Asymmetry* **1998**, *9*, 3997–4008; b) M. I.; Burguete, J. M. Fraile, J. I. García, E. García-Verdugo, C. I. Herrerías, S. V. Luis, J. A. Mayoral, *J. Org. Chem.* **2001**, *66*, 8893–8901; c) A. Cornejo, J. M. Fraile, J. I. García, M. J. Gil, G. Legarreta, S. V. Luis, V. Martínez-Merino, J. A. Mayoral, *Org. Lett.* **2002**, *4*, 3927–3930.
[13] J. M. Fraile, J. I. García, J. A. Mayoral, T. Tarnai, *J. Mol. Catal. A* **1999**, *144*, 85–89.
[14] J. M. Fraile, J. I. García, J. A. Mayoral, T. Tarnai, M. A. Harmer, *J. Catal.* **1999**, *186*, 214–221.
[15] J. M. Fraile, J. I. García, V. Martínez-Merino, J. A. Mayoral, L. Salvatella, *J. Am. Chem. Soc.* **2001**, *123*, 7616–7625.
[16] M. Bühl, F. Terstegen, F. Löffler, B. Meynhardt, S. Kierse, M. Müller, C. Näther, U. Lüning, *Eur. J. Org. Chem.* **2001**, 2151–2160.
[17] T. Rasmussen, J. F. Jensen, N. Østergaard, D. Tanner, T. Ziegler, P.-O. Norrby, *Chem. Eur. J.* **2002**, *8*, 177–184.
[18] D. A. Evans, K. A. Woerpel, M. J. Scott, *Angew. Chem.* **1992**, *104*, 439–441; *Angew. Chem. Int. Ed. Engl.* **1992**, *31*, 430–432.
[19] a) C. Lee, W. Yang, R. Parr, *Phys. Rev. B* **1988**, *37*, 785–789; b) A. D. Becke, *J. Chem. Phys.* **1993**, *98*, 5648–5652.
[20] S. Niu, M. B. Hall, *Chem. Rev.* **2000**, *100*, 353–406.
[21] M. J. Frisch, G. W. Trucks, H. B. Schlegel, G. E. Scuseria, M. A. Robb, J. R. Cheeseman, V. G. Zakrzewski, J. A. Montgomery Jr., R. E. Stratmann, J. C. Burant, S. Dapprich, J. M. Millan, A. D. Daniels, K. N. Kudin, M. C. Strain, O. Farkas, J. Tomasi, V. Barone, M. Cossi, R. Cammi, B. Mennucci, C. Pomelli, C. Adamo, S. Clifford, J. Ochterski, G. A. Petersson, P. Y. Ayala, Q. Cui, K. Morokuma, D. K. Malick, A. D. Rabuck, K. Raghavachari, J. B. Foresman, J. Cioslowski, J. V. Ortiz, B. B. Stefanov, G. Liu, A. Liashenko, P. Piskorz, I. Komaroni, R. Gomperts, R. L. Martin, D. J. Fox, T. Keith, M. A. Al-Laham, C. Y. Peng, A. Nanayakkara, C. González, M. Challacombe, P. M. W. Gill, B. Johnson, W. Chen, E. S. Replogle, J. A. Pople, Gaussian 98, Revisions A.7 and A.11; Gaussian, Inc., Pittsburgh (PA), **1998**.
[22] C. W. Bauschlicher Jr. , *Chem. Phys. Lett.* **1995**, *246*, 40–44.
[23] J. B. Foresman, T. A. Keith, K. B. Wiberg, J. Snoonian, M. J. Frisch, *J. Phys. Chem.* **1996**, *100*, 16098–16104.
[24] B. F. Straub, P. Hofmann, *Angew. Chem.* **2001**, *113*, 1328–1330; *Angew. Chem. Int. Ed.* **2001**, *40*, 1288–1290.
[25] a) F. Bernardi, A. Bottoni, G. P. Miscione, *J. Am. Chem. Soc.* **1997**, *119*, 12300–12305; b) A. Hirai, M. Nakamura, E. Nakamura, *Chem. Lett.* **1998**, 927–928; c) H. Hermann, J. C. W. Lohrenz, A. Kühn, G. Boche, *Tetrahedron* **2000**, *56*, 4109–4115; d) W.-H. Fang, D. L. Phillips, D. Wang, Y.-L- Li, *J. Org. Chem.* **2002**, *67*, 154–160.
[26] a) R. G. Salomon, J. K. Kochi, *J. Am. Chem. Soc.* **1973**, *95*, 3300–3310; b) M. M. Díaz-Requejo, T. R. Belderrain, M. C. Nicasio, F. Prieto, P. J. Pérez, *Organometallics* **1999**, *18*, 2601–2609.

Received: May 20, 2003
Revised: October 6, 2003 [F5161]

